



Employing Gaussian Apodization Technique in Fiber Bragg Gratings: A Simulation Study

M. Mahdi Shahidi^{1*}, Ali A. Orouji², SO. Mohammadi² and Nasrin Salehi¹

¹Department of Basic Sciences, Shahrood Branch, Islamic Azad University, Shahrood, Iran.

²Electrical Engineering Department, Semnan University, Semnan, Iran.

Authors' contributions

This work was carried out in collaboration between all authors. Author MMS designed the study, performed the statistical analysis, wrote the protocol, and author SM wrote the first draft of the manuscript. Author AAO managed the analyses of the study. Author NS managed the literature searches. All authors read and approved the final manuscript.

Research Article

Received 12th March 2013
Accepted 7th September 2013
Published 16th October 2013

ABSTRACT

Nowadays, by increasingly using the Dense Wave Division Multiplexing (DWDM) in communication industry, Fiber Bragg Gratings (FBGs) are extensively used in various telecommunication and sensors because of adjustable properties of Bragg wavelength and their bandwidth. In this article, numerical simulation of optical fiber and FBGs is done based on three dimensional algorithm of Finite Difference Time Domain (FDTD). Using this method, propagation of a wave in an optical fiber and a uniform FBG are shown and the results are compared with employing Gaussian apodization on index profile of FBG. Our results show the efficiency of FBGs improves.

Keywords: FBG; FDTD; apodization; simulation.

1. INTRODUCTION

Discovery of optical sensing creates a novel part of in-fiber components named Fiber Bragg Gratings (FBG). FBGs were an evolution in communication and optical fiber sensors. This device does operation like reflection and filtering in optical fiber with high efficiency and low

*Corresponding author: Email: mmahdishahidi@gmail.com;

dissipation. FBGs simply include a periodic structure of refractive index variation in optical fiber core. Also these structures are used for optical filtering and coupling in waveguides [1].

FBG is a type of Bragg reflectors which is created in a small part of core of optical fiber, and reflects specific wavelengths and transmits others. This structure is resulted with periodic variation in refractive index of core that acts like a mirror for a specific wavelength. FBG can be also utilized as an inner optical fiber in order to stop definite wavelength or as a reflector for particular wavelengths [2]. These devices follow the Fresnel reflection law; according to this law both reflection and transmission between two medium happen when light arrives to a medium with different refractive index. Gratings, usually, have sinusoidal variation for refractive index of a particular length. Reflected wavelength called Bragg wavelength (λ_B) and is given by:

$$\lambda_B = 2n\Lambda \quad (1)$$

Where n is effective refractive index of grating in core and Λ is grating period [2].

The reflectivity increases with increase in grating length and also refractive index difference. On the other hand, strength of side lobes in reflectivity curve of uniform FBG increases with increase of grating length and index difference. To reduce this, apodization can be applied. The grating apodization profiles are described as a function of spatial distance as Gaussian, Sinc, etc. [3]. The immediate impact of apodization on gratings is the remarkable reduction in the side-lobe levels in the reflection spectrum. Another benefit of apodization is in the reduction of internal interference effects that cause the group delay to obtain a ripple.

One of the important approaches used for numerical simulation of the dynamics of the electromagnetic fields in waveguides is the FDTD method which is now among the most popular numerical schemes for study field distribution and wave propagation in various media [4,5]. The advantages of the FDTD method are its comparative simplicity and calculating ability electromagnetic wave propagation in media with almost complex properties. When the FDTD is applied, the investigated domain is covered with the separate grid, which form is defined by the geometry of the studied system. Both time and space components for electric and magnetic fields are moved from each other for the half step of discretization that provides the precision of numerical calculation of the second order. To simulate the open system we use boundary conditions in a form of Convolutional Perfectly Matched Layer (CPML). This approach provides all descending waves to penetrate into the layers without reflection and dissipate further within the CPML [5].

2. OPTICAL FIBER SIMULATION

In this article, FDTD algorithm, which was firstly proposed by Yee, is applied [6]. Fig. 1 shows a schematic of single-mode optical fiber. Radius of fiber core is $a=4.5\mu\text{m}$ and refractive index of core and cladding of fiber are $n_1=1.45$ and $n_2=1.43$, respectively. In a fiber core permittivity is given as follow:

$$\epsilon_{r1} = (n_1)^2 \quad (2)$$

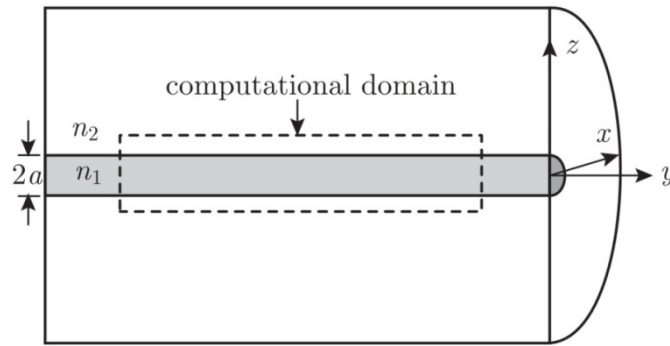


Fig. 1. Schematic image of single-mode optical fiber

Domain of simulation is offered in cubic shape, because electric field of propagated light mostly distributes in the fiber core. Dimensions of simulation region are $-9\mu\text{m} \leq x \leq 9\mu\text{m}$, $-9\mu\text{m} \leq z \leq 9\mu\text{m}$ and $0 \leq y \leq 10\mu\text{m}$, the lattice grid size is $\Delta=0.1\mu\text{m}$. In order to decrease the reflection in boundaries, CPML with 8 cells thickness is used as a boundary condition (Fig. 2) [7].

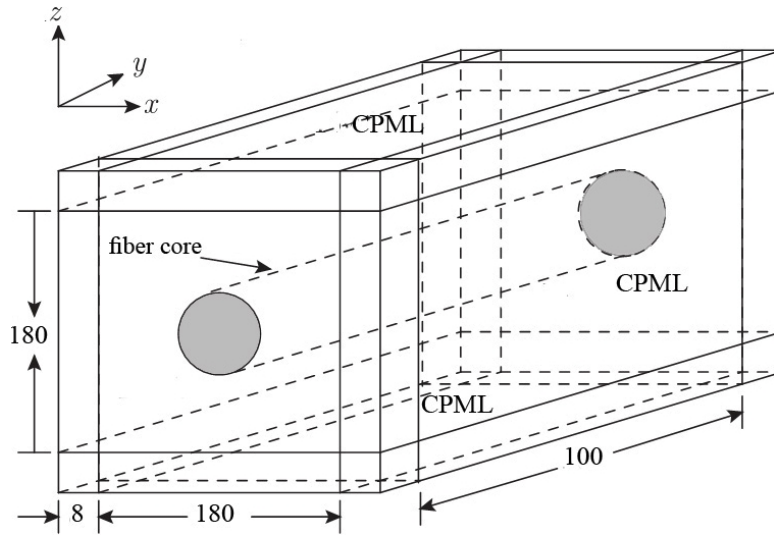


Fig. 2. FDTD simulation domain

To insure the stability of the time stepping algorithm Δt is chosen to satisfy

$$\Delta t \leq \Delta / V_{\text{max}} \tag{3}$$

Where $V_{\text{max}}=c/n_2$ is maximum phase velocity of light in simulation domain [6]. We choose time growth as $\Delta t=\Delta/4V_{\text{max}}$. After computing V_{max} and considering the velocity of light in vacuum, time growth is achieved equal to 1.873×10^{-16} s. In FDTD algorithm time is defined as $t=n\Delta t$ in which n denotes the time. When the simulation starts ($n=0$), a light pulse appears at $0 \leq y \leq 6\mu\text{m}$. The electrical fields of incident beam are assumed to include E_z component only:

$$E_z^0(x,y,z) = 1/2 [1 - \cos(2\pi y/L)] \times \exp[-(x^2 + y^2)/a^2] \quad (4)$$

Electric and magnetic fields for $n > 0$ is calculated with FDTD algorithm as soon as a light pulse propagate into fiber. Figs. 3, 4, and 5 illustrate the E_z for $n=100$, $n=150$ and $n=200$. In these figures, the light pulse propagates along $+y$, and as it shown, incident wave diminishes because wave radiates into cladding. Incident pulse includes both propagation and radiation modes.

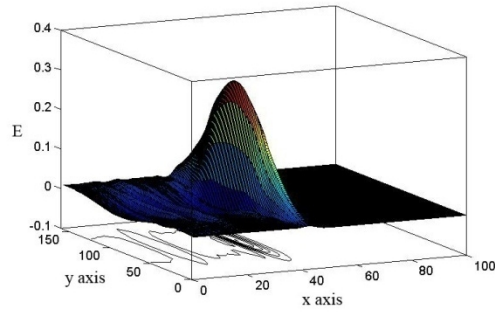


Fig. 3. E_z at xy plane for $n=100$

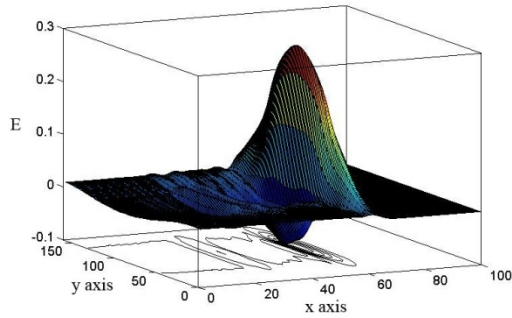


Fig. 4. E_z at xy plane for $n=150$

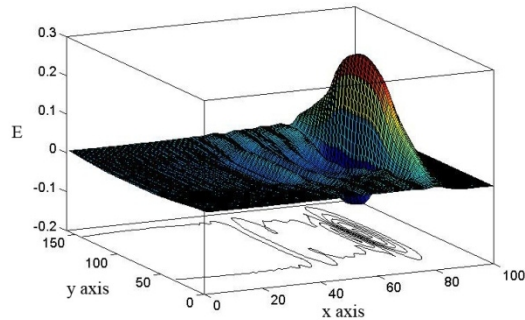


Fig. 5. E_z at xy plane for $n=200$

3. FBG SIMULATION

A schematic image of FBG is shown in Fig. 6. Refractive index variations in fiber core is expected to be as

$$\Delta n_1(y) = \Delta n [1 + \cos(2\pi y/\Lambda)] \tag{5}$$

In this equation, Δn the amplitude of refractive index variation which we assume 5×10^{-4} . Λ is grating period that is $0.535 \mu\text{m}$ in simulation. According to this period, Bragg wavelength of simulated grating is computed near $1.55 \mu\text{m}$ (equation 1).

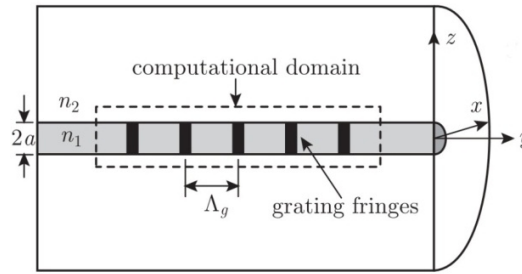


Fig. 6. Schematic image of FBG

Refractive index core and electric permittivity of core will be as

$$n_1(y) = n_1 + \Delta n_1(y) \tag{6}$$

$$\epsilon_{r1}(y) = [n_1(y)]^2 \tag{7}$$

For $\Delta n \ll n_1$, above equation will be as

$$\epsilon_{r1}(y) \approx (n_1)^2 + 2n_1 \Delta n_1(y) \tag{8}$$

We consider the computation domain of FBG simulation like previous part and define the incident pulse according to Eq. (4). This simulation is similar to optical fiber except the fiber core that has 16 periods. Reflecting wave is so weak that it is not visible in comparison to propagating wave. In order to indicate the reflected wave, we have simulated optical fiber and Bragg grating, simultaneously. We also obtain the dE_z between optical fiber and Bragg grating in time step, n .

$$dE_z^n(x,y,z) = E_z^n(x,y,z) \Big|_{\text{grating}} - E_z^n(x,y,z) \Big|_{\text{fiber}} \tag{9}$$

That dE_z is computed for $n=100$, $n=150$ and $n=200$.

Then we have used Gaussian apodization to reduce side lobes reflectivity. In these gratings refractive index in core follows this equation [8]:

$$\Delta n_1(y) = \exp(-y^2/a^2) \Delta n [1 + \cos(2\pi y/\Lambda)] \tag{10}$$

Like uniform FBG, dE_z for $n=100$, $n=150$ and $n=200$ is computed.

At $n > 100$; 150 and 200, the dE_z component of electric field at xy plane are displayed in Figs. 7-9, respectively. As can be seen from the figures, distortion is reduced by applying Gaussian apodization. Contours in Figs. 7-9(b) indicate undesirable interference of reflected wave. It results that apodization techniques optimize the reflection spectra.

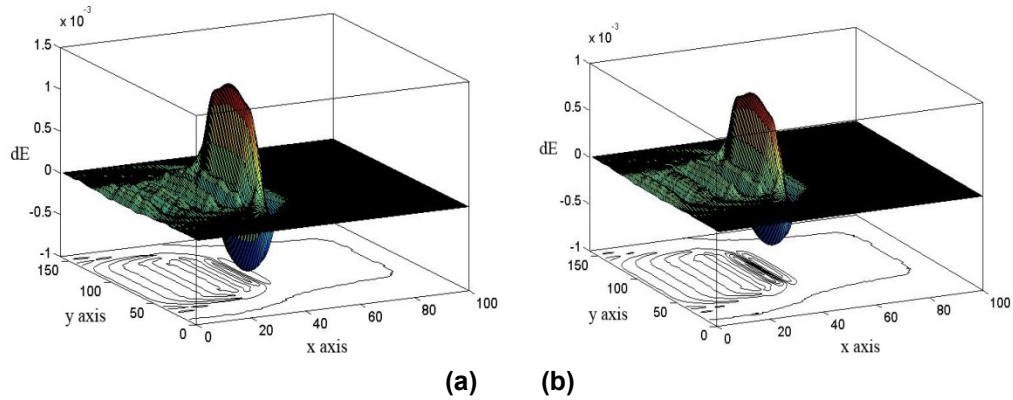


Fig. 7. dE_z at xy plane for $n=100$ (a) without apodization, (b) with apodization

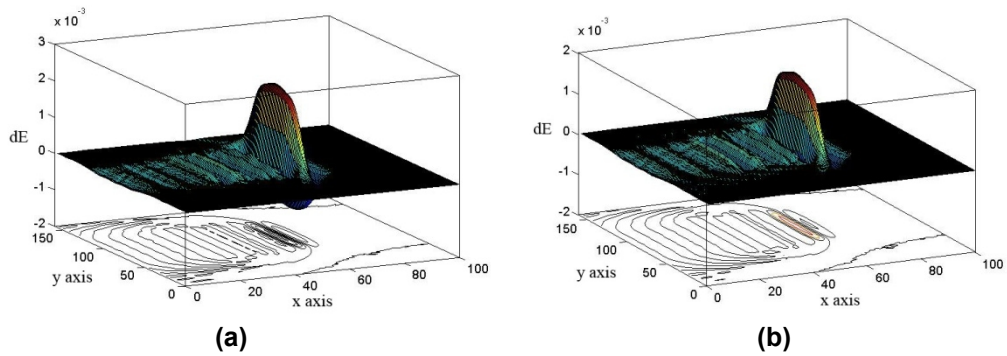


Fig. 8. dE_z at xy plane for $n=150$ (a) without apodization, (b) with apodization

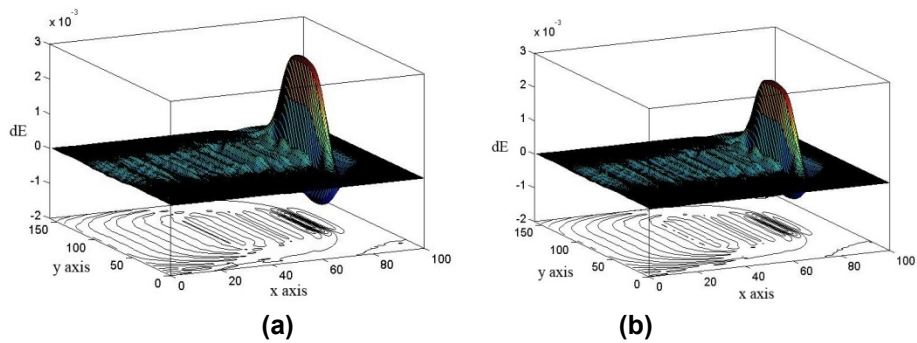


Fig. 9. dE_z at xy plane for $n=200$ (a) without apodization, (b) with apodization.

4. TILT FBG SIMULATION

Fig. 10 shows a schematic image of tilt FBG. To illustrate an inclined grating, the coordinate should rotate around x axis. In new coordinate the z axis is described as follow:

$$\tilde{y} = y \cos\theta - x \sin\theta \tag{11}$$

Refractive index variation is defined by substituting above equation in equation (5):

$$\Delta n_1(y) = \Delta n \{ 1 + \cos [(2\pi y/\Lambda)(y \cos\theta - x \sin\theta)] \} \tag{12}$$

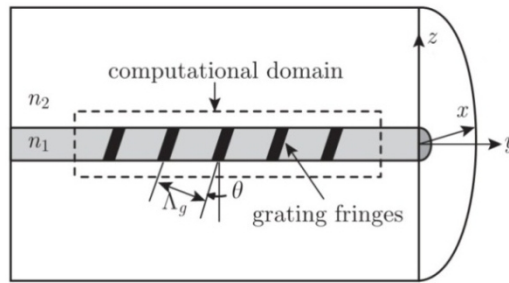


Fig. 10. Schematic image of tilt FBG

In this simulation, we have chosen the amount of 18 for θ . Parameter in this profile is like previous one and incident pulse is defined according to Eq. (4). Both optical fiber and tilt FBG simulation were done simultaneously. Finally, difference of various amounts of n (dE_z) has computed in these two simulations.

To diminish the side lobes reflectivity we applied the Gaussian apodization in tilt profile. Bellow equation shows differences of refractive index in simulation.

$$\Delta n_1(y) = \exp(-y^2/a^2) \Delta n \{ 1 + \cos [(2\pi y/\Lambda)(y \cos\theta - x \sin\theta)] \} \tag{13}$$

Figs. 11-13 depict the dE_z in tilt profile for $n=100$, $n=150$ and $n=200$, considering the apodization and without it.

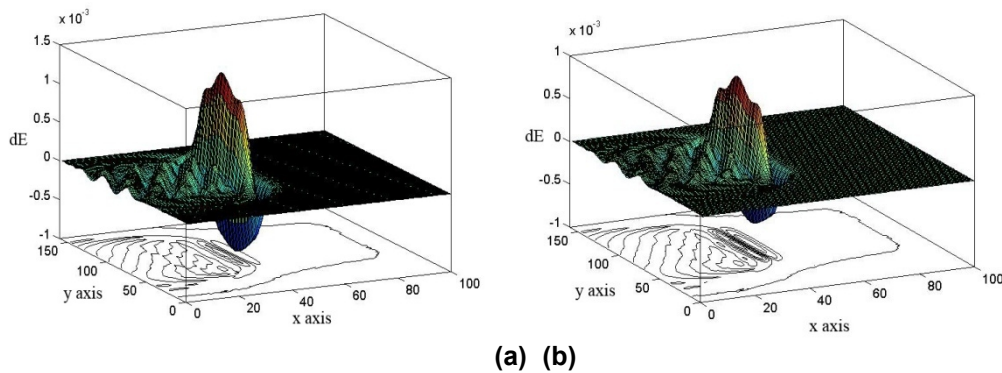


Fig. 11. dE_z at xy plane for $n=100$ (a) without apodization, (b) with apodization

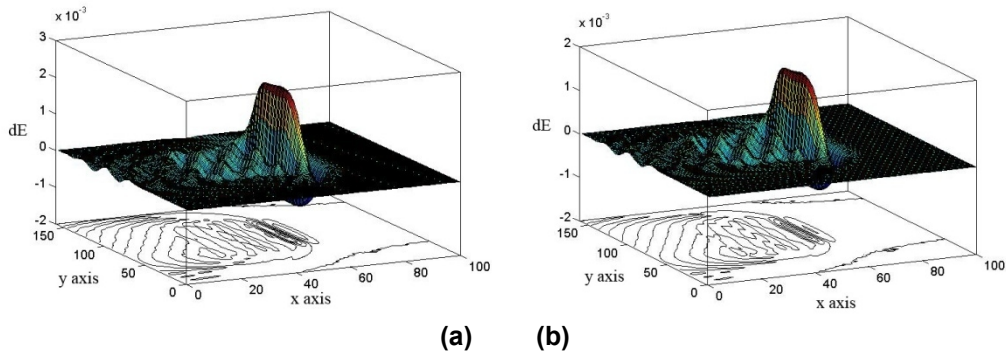


Fig. 12. dE_z at xy plane for $n=150$ (a) without apodization, (b) with apodization

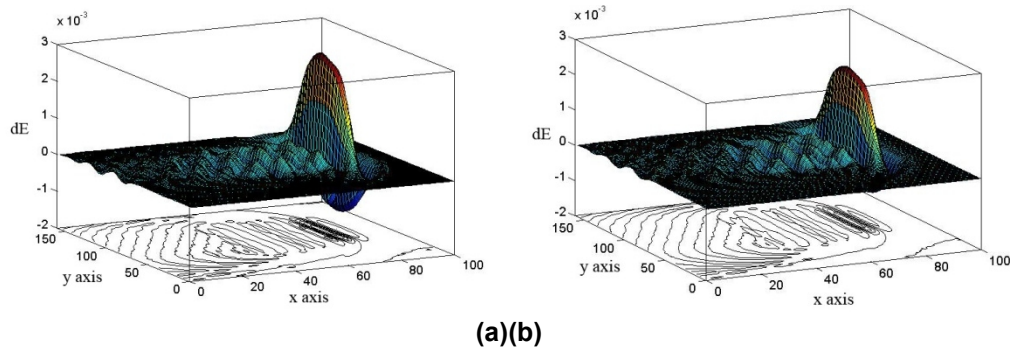


Fig. 13. dE_z at xy plane for $n=200$ (a) without apodization, (b) with apodization

As can be seen from the figures, distortion is reduced remarkably in apodization tilt, and reflected wave is also separable. Interference in reflected wave is reduced by declining side lobes that result to improve the efficiency of FBG.

5. CONCLUSION

Wave propagating in optical fiber, Bragg grating and tilt FBG were simulated based on three dimensional FDTD. Then its results compare with applying of Gaussian apodization. We have shown that by taking advantages of apodization, the efficiency of FBG is enhanced.

COMPETING INTERESTS

Authors have declared that no competing interests exist.

REFERENCES

1. Othonos A, Kyriacos K. Fiber Bragg Grating: Fundamentals and Application in telecommunication and Sensing, Artech House, Boston; 1999.
2. Kashyap R. Fiber Bragg Gratings. 2nd ed. Academic Press; 2009.

3. Ugale S, Mishra V. Fiber Bragg Grating modeling, Characterization and Optimization with different index profiles. *International Journal of Engineering Science and Technology*. 2010;2(9):4463-4468.
4. Taflove A, Brodwin M. Numerical Solution of Steady-State Electromagnetic Scattering Problems Using the Time-Dependent Maxwell's Equations. *IEEE Trans. Microwave Theory Tech*. 1975;23:623-630.
5. Taflove A, Susan C. Hagness. *Computational Electrodynamics the Finite-Difference Time-Domain Method*. 3rd ed. Artech House; 2005.
6. Yee K. Numerical solution of initial boundary value problems involving maxwell's equations in isotropic media. *IEEE Trans. Antennas Propag*. 1966;14:302-307.
7. Roden, JA, Gedney SD. Convolutional PML (CPML): an efficient FDTD implementation of the CFS-PML for arbitrary media. *Microw. Opt. Technol. Lett*. 2000;27:334-339.
8. Ho SzePhing, et al. Fiber Bragg grating modeling, simulation and characteristics with different grating lengths. *Malaysian Journal of Fundamental and Applied Sciences*. 2007;3:167-175.

© 2014 Shahidi et al.; This is an Open Access article distributed under the terms of the Creative Commons Attribution License (<http://creativecommons.org/licenses/by/3.0>), which permits unrestricted use, distribution, and reproduction in any medium, provided the original work is properly cited.

Peer-review history:

The peer review history for this paper can be accessed here:
<http://www.sciencedomain.org/review-history.php?iid=283&id=4&aid=2270>